Molecular Therapy
Nucleic Acids
Original Article

Nanoblades allow high-level genome editing in murine and human organoids

Victor Tiroille,[1,12,14] Adrien Krug,[1,14] Emma Bokobza,[1,12] Michel Kahi,[1,12] Mattijs Bulcaen,[3,4] Marjolein M. Ensinck,[3,4] Maarten H. Geurts,[5,6] Delilah Hendriks,[5,6] François Vermeulen,[7] Frédéric Larbret,[1] Alejandra Gutierrez-Guerrero,[2] Yu Chen,[8] Indra Van Zundert,[9] Susana Rocha,[10] Anne C. Rios,[6,11] Louise Medaer,[3] Rik Gijsbers,[3] Philippe E. Mangeot,[2] Hans Clevers,[5,6,13] Marianne S. Carlon,[3,4] Frédéric Bost,[1,12] and Els Verhoeyen[1,2]

[1]Université Côte d'Azur, INSERM, C3M, 06204 Nice, France; [2]CIRI – International Center for Infectiology Research, Inserm, U1111, Université Claude Bernard Lyon 1, CNRS, UMR5308, Ecole Normale Supérieure de Lyon, Université Lyon, F-69007 Lyon, France; [3]Laboratory for Molecular Virology and Gene Therapy, Department of Pharmaceutical and Pharmacological Sciences, Faculty of Medicine, KU Leuven, Leuven, Belgium; [4]Laboratory of Respiratory Diseases and Thoracic Surgery (BREATHE), Department of Chronic Diseases and Metabolism, KU Leuven, Leuven, Belgium; [5]Hubrecht Institute, Royal Netherlands Academy of Arts and Sciences (KNAW) and University Medical Center Utrecht, Utrecht, the Netherlands; [6]Oncode Institute, Hubrecht Institute, Utrecht, the Netherlands; [7]UZ Leuven, Department of Pediatrics, Leuven, Belgium; [8]Human Oncology and Pathogenesis Program, Department of Medicine, Memorial Sloan; Department of Medicine, Weill Cornell Medical College, New York, NY 10065, USA; [9]Synthetic Biology Group, Department of Biomedical Engineering, Eindhoven University of Technology, P.O. Box 513, 5600 MB Eindhoven, the Netherlands; [10]Molecular Imaging and Photonics, Department of Chemistry, KU Leuven, Celestijnenlaan 200F, 3001 Heverlee, Belgium; [11]Princess Máxima Center for Pediatric Oncology, Utrecht, the Netherlands; [12]Equipe labélisée Ligue National Contre le Cancer, Basel, Switzerland

Genome engineering has become more accessible thanks to the CRISPR-Cas9 gene-editing system. However, using this technology in synthetic organs called "organoids" is still very inefficient. This is due to the delivery methods for the CRISPR-Cas9 machinery, which include electroporation of CRISPR-Cas9 DNA, mRNA, or ribonucleoproteins containing the Cas9-gRNA complex. However, these procedures are quite toxic for the organoids. Here, we describe the use of the "nanoblade (NB)" technology, which outperformed by far gene-editing levels achieved to date for murine- and human tissue-derived organoids. We reached up to 75% of reporter gene knockout in organoids after treatment with NBs. Indeed, high-level NB-mediated knockout for the androgen receptor encoding gene and the cystic fibrosis transmembrane conductance regulator gene was achieved with single gRNA or dual gRNA containing NBs in murine prostate and colon organoids. Likewise, NBs achieved 20%–50% gene editing in human organoids. Most importantly, in contrast to other gene-editing methods, this was obtained without toxicity for the organoids. Only 4 weeks are required to obtain stable gene knockout in organoids and NBs simplify and allow rapid genome editing in organoids with little to no side effects including unwanted insertion/deletions in off-target sites thanks to transient Cas9/RNP expression.

INTRODUCTION

Organoids are self-organized three-dimensional culture systems derived from embryonic stem cells, adult stem cells (ASCs), or induced pluripotent stem cells (iPSCs).[1–4] They recapitulate architecture, composition, and functionality of their original epithelial tissues more faithfully than the traditionally used two-dimensional immortalized cell lines.[5,6] This model can be used to study stem cell differentiation, gene therapy approaches, and spatial organization processes.[7] Thus, organoid technology is ideal for deciphering the role of genes involved in organogenesis or human pathologies.[8,9] Therefore, efficient approaches to edit the genome of mouse tissue-derived organoids and organoids derived from human ASCs are urgently required.[10–15]

Gene editing consists in manipulating the genome to induce gene silencing, gene modification, or transgene integration at a precise locus.[16] In contrast to ectopic DNA sequence insertion using integrative vectors, genome editing allows more physiological gene manipulation. Precise genome editing also avoids gene silencing of non-targeted genes and adverse mutagenic effects such as insertional mutagenesis. Gene editing is based on the induction of double-strand breaks (DSBs) at a precise locus.[17] For some time now, the clustered regularly interspaced short palindromic repeats (CRISPR)-associated protein 9 (Cas9) technology has been introduced in the field.[16] This system relies on an endonuclease that uses a single-guide RNA sequence (sgRNA) to introduce a site-specific DSB in the targeted DNA. The most common repair that occurs after a DSB is non-homologous end joining (NHEJ). This consists in the fusion of the

Received 8 December 2022; accepted 4 June 2023;
https://doi.org/10.1016/j.omtn.2023.06.004.

[13]Present address: Pharma Research Early Development, Roche, Basel, Switzerland

[14]These authors contributed equally

Correspondence: Frédéric Bost, Université Côte d'Azur, INSERM, C3M, 06204 Nice, France.
E-mail: Frederic.BOST@univ-cotedazur.fr
Correspondence: Els Verhoeyen, Université Côte d'Azur, INSERM, C3M, 06204 Nice, France.
E-mail: els.verhoeyen@unice.fr

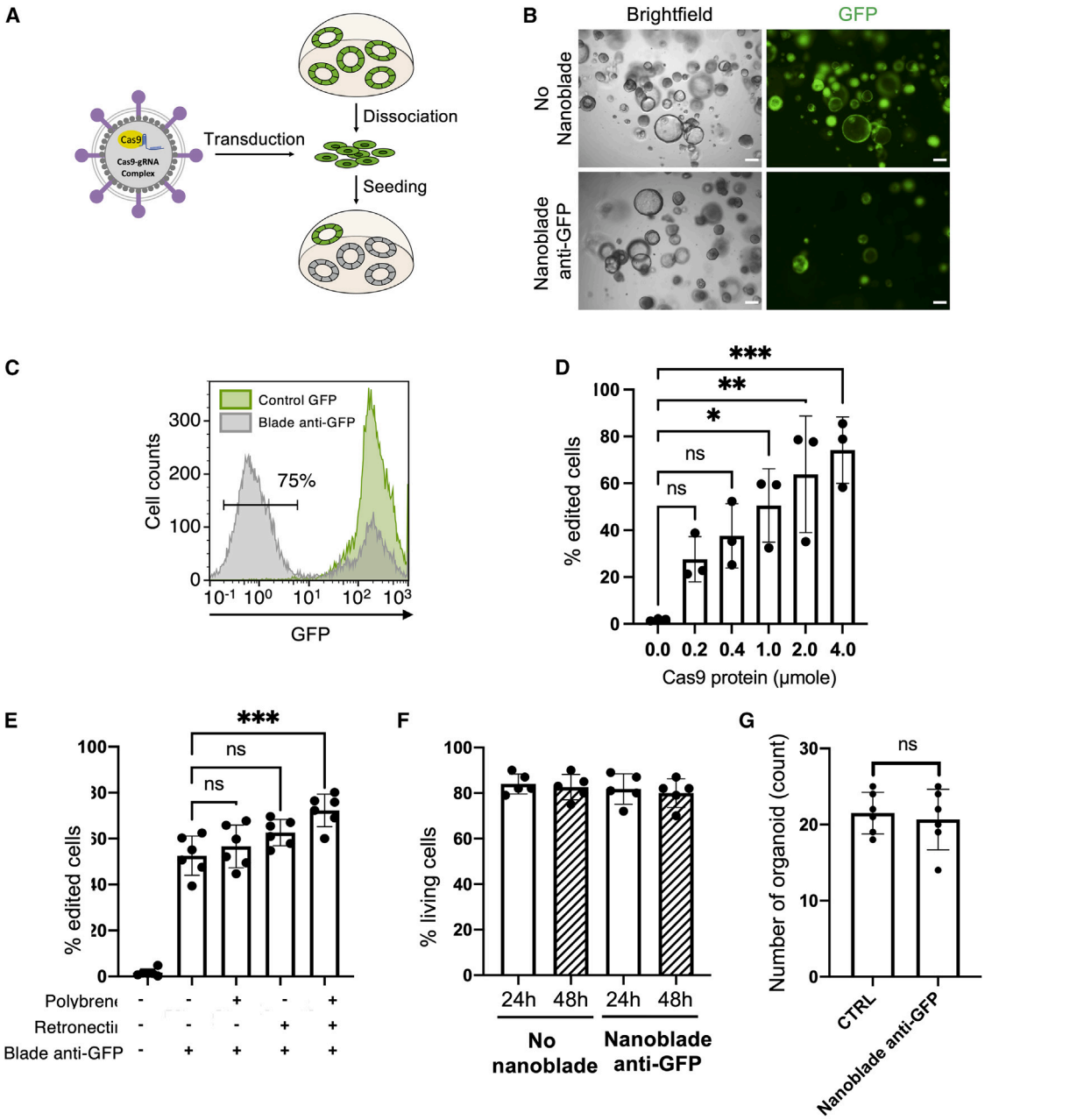

(legend on next page)

two DNA ends and can lead to the insertion or deletion of a few base pairs (INDELs). The frame shifts induced by these INDELs will modify partially or totally gene transcription and translation. Alternatively, homology-directed repair can occur when a donor sequence, with locus-specific homology arms, is available in addition to the endonuclease. This allows the introduction of a specific DNA alteration such as single-base substitution and also insertion of site-specific ectopic DNA sequences to correct a mutated gene.[18]

The CRISPR-Cas9 technology has revolutionized the methodology to induce gene-specific knockouts (KOs) due to its high specificity, easy design, and high efficiency in genetic manipulation of cell lines and primary cells. Endonucleases and sgRNAs can be introduced in the cell by using CRISPR-Cas9- and sgRNA-encoding retroviral vectors.[19] Alternatively, electroporation of plasmids or mRNA encoding the Cas9 have also been used.[20,21] The main approach used in ASC-derived organoids is still electroporation of plasmids coding for the Cas9 endonuclease and the sgRNA.[11] Despite that, electroporation is widely used today; this technique leads to low gene-editing efficiency and induces a high level of cell death.[11,13] Nevertheless, a recent study reported that the electroporation of ribonucleoprotein (RNP), combining Cas9 protein and a synthetic single-strand gRNA, provided higher gene-editing efficiency into cells.[22]

Gene editing has already been performed in several types of organoids such as rectal organoids. Cystic fibrosis transmembrane conductance regulator (CFTR) is an integral membrane protein that forms an anion channel activated by cAMP-dependent phosphorylation.[23] A study published in 2013 reported the use of the CRISPR-Cas9 genome-editing system to correct the *CFTR* gene in patient-derived intestinal rectal organoids.[10]

Androgenic signals through the androgen receptor (AR) are required for luminal differentiation of some prostate basal stem cells. The first study that established prostate organoid cultures[24] showed that dihydrotestosterone (DHT) deprivation of CD26+ luminal cell-derived organoids disrupted lumen formation. Therefore, *AR* KO prostate organoids generated by gene editing are expected to be compact even when stimulated with DHT. Therefore, both *CFTR* and *AR* are model target genes to evaluate gene editing in organoids.

Recently, a gene-editing tool called nanoblades (NBs), based on a virus-like particle (VLP) derived from a murine leukemia virus (MLV), has been developed.[25–27] This technology uses the VLPs to introduce the Cas9/sgRNA RNPs into cells. These NBs carry the Cas9 proteins complexed with the sgRNAs, and are devoid of a viral genome, which allows a very quick and transient delivery of the gene-editing machinery into the targeted cells. Here, we demonstrated that NBs allowed a very high gene-editing efficiency for *AR* and *CFTR* in murine prostate and both murine and human rectal organoids, respectively. Moreover, this editing efficiency was accompanied by low toxicity and no obvious off-target effects. This facilitates the generation of gene KO in organoids since it does not require the use of a reporter encoding knockin cassette to facilitate KO detection.

RESULTS

NBs allow efficient genome editing in organoid cells with low toxicity

As an easy readout for NB gene-editing efficiency in organoids, we chose initially to knock out eGFP in prostate organoids expressing eGFP. First, we established a mouse prostate organoid cell line expressing eGFP. Organoid cells were transduced with a lentiviral vector (LV) encoding eGFP driven by the SFFV promoter at low vector doses (MOI = 0.3) to ensure only one integrated copy of the eGFP expression cassette per organoid cell. The eGFP+ cells were sorted to establish the eGFP organoid cell line.

To assess eGFP KO, we selected a sgRNA targeting eGFP that previously resulted in 75% of eGFP KO in bone marrow-derived macrophages.[25] The NB treatment is schematically represented in Figure 1A. Organoids were dissociated and incubated with the NBs for only 6 h. Of note, absence of growth factors for more than 6 h induced cell death. Moreover, a brief incubation with NBs was expected to be sufficient since receptor-mediated entry of the NBs is a fast process, as shown previously for other primary cells.[25,26] The cells were then rinsed to remove the NBs and seeded in Matrigel. Without any prior selection for gene-edited cells, the single-cell suspension was grown for 9 days into organoids. Fluorescence microscopy revealed a strong reduction of eGFP+ organoids (Figure 1B). In addition, the bulk population of dissociated organoids was quantified by FACS for NB-mediated loss of eGFP expression. For example, 75% of the cells lost their GFP expression (Figure 1C). We observed that increasing

Figure 1. Strategy and efficiency of NB-induced KO in mouse prostate organoids

(A) Experimental workflow using NBs for gene editing of mouse prostate organoids. Organoids are dissociated, treated with the NBs, and seeded back into Matrigel supplemented with growth factors inducing organoid generation. (B) Representative bright-field images of mouse prostate organoids 9 days after treatment with or without NBs targeting the eGFP coding sequence. Scale bar, 200 μm. (C) Flow cytometry analysis of eGFP-expressing organoids treated or not with NBs targeting the GFP coding sequence. (D) Flow cytometry analysis of eGFP-expressing organoids treated with different quantities of anti-GFP NBs, the percent of GFP− cells indicates the percent of editing cells (means ± SD, n = 3, biological replicates, one-way ANOVA, Tukey's multiple comparisons test; *$p < 0.05$, **$p < 0.01$, ***$p < 0.001$). (E) Flow cytometry analysis of eGFP-expressing organoids treated with fixed amounts of anti-GFP NBs (1 μmol Cas9) with or without polybrene and/or retronectin (means ± SD, n = 6, biological replicates, one-way ANOVA, Tukey's multiple comparisons test; ***$p < 0.001$; ns, not significant). (F) FACS analysis for living prostate organoid cells (DAPI+) 24 or 48 h after incubation or not with NBs (means ± SD, n = 6, biological replicates, t test, Mann-Whitney test, non-parametric, not significant). (G) The toxicity in organoids was evaluated, 9 days after incubation of organoid cells with or without NBs by counting of the number of organoids developing per fixed number of cells seeded (means ± SD, n = 6, biological replicates, t test, Mann-Whitney test, non-parametric, not significant). (H) Immunofluorescence images of mouse prostate organoids treated or not with NBs. Stainings were performed for the basal cell marker CK5 (cyan), luminal cells marker CK8 (red), and AR (green). Scale bar, 100 μm. Images are representative of n = 4.

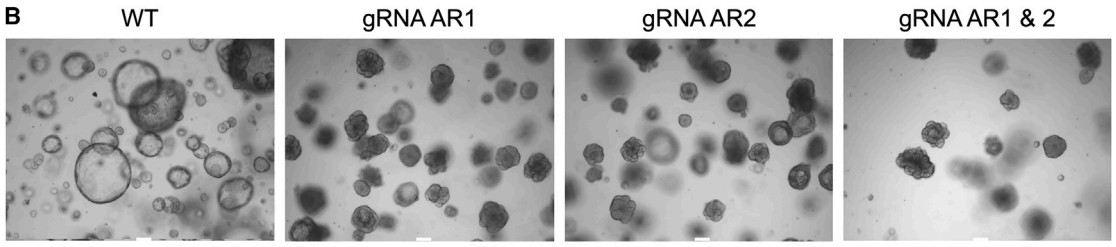

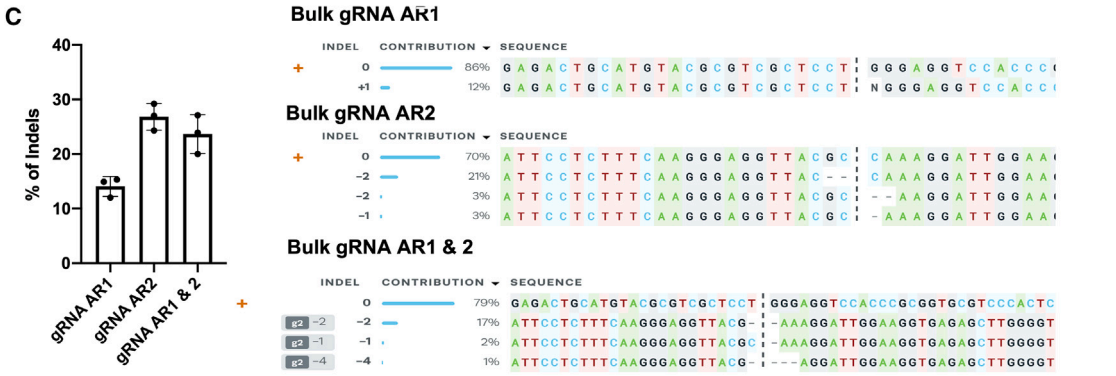

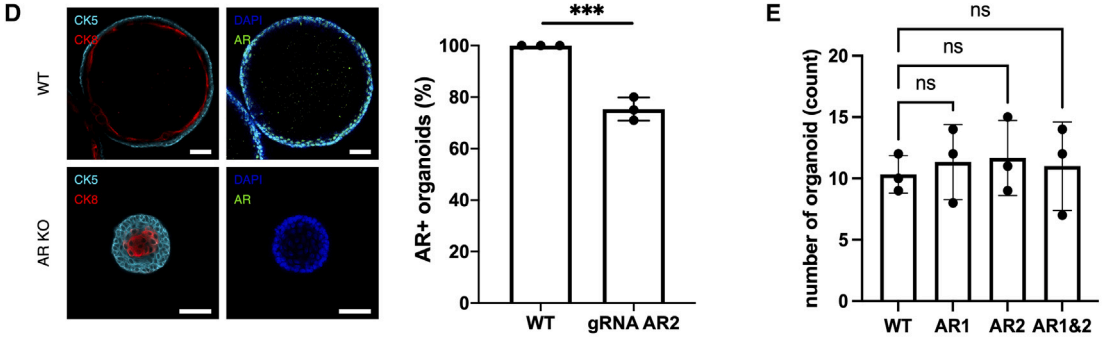

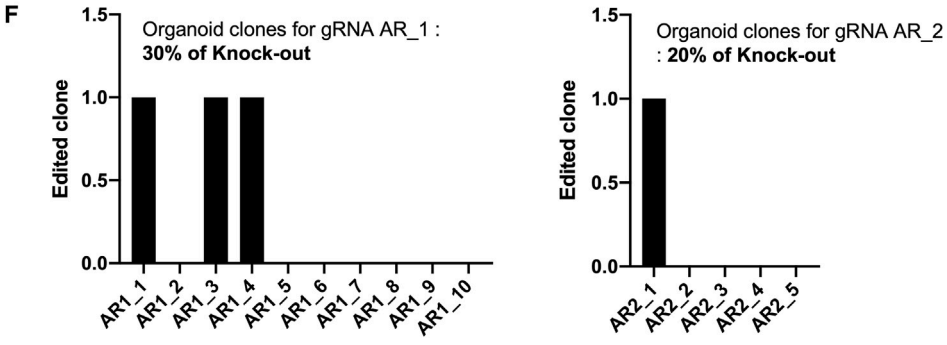

(legend on next page)

doses of anti-GFP NBs permitted to increase gene editing and resulted in up to 80% gene-edited cells when the highest doses of NBs was applied (Figure 1D).

To further improve the efficiency of NBs, we compared a constant dose of NBs in combination with two transduction facilitating agents, polybrene and/or retronectin (Figure 1E).[28] A significant increase in gene-editing efficiency using NBs was only observed in the presence of retronectin and polybrene compared with the control condition in absence of these facilitating agents. Short-term toxicity was evaluated by DAPI staining 24 and 48 h after NB incubation or not. NBs did not increase cell death compared with the control (Figure 1F). Of high importance, even after treatment of dissociated organoid cells with the maximum dose of NBs tested (4 μmol of Cas9 protein), no significant toxicity was detected since the number of cells developing into organoids was equivalent in the presence or absence of NB incubation (Figure 1G). Moreover, the size distribution and the structure of the organoids did not change after anti-GFP NB incubation (Figures S1 and 1H). These data suggested that NBs can reach high-level gene editing in organoids without toxic side effects such as cellular toxicity.

NBs allow highly efficient gene KO in mouse prostate organoids

As a proof of concept, we chose to knock out the gene coding for the AR, a key protein in the development of mouse prostate and prostate organoids. Therefore, we designed two sgRNAs targeting exon 1 or exon 8 in the *AR* locus. The experimental setup is shown in Figure 2A and as indicated can be performed in 4–6 weeks to obtain organoid KO for a specific gene. The layout of the experiment includes cloning of the gRNA in an RNA expression plasmid, followed by the NB production carrying the *AR*-targeted sgRNAs. Furthermore, dissociated mouse prostate wild-type (WT) organoids were treated either with the NBs carrying the AR_1 sgRNA or the AR_2 sgRNA or both sgRNAs simultaneously. After 9 days of organoid culture, we revealed a strong phenotypic change in the organoid KO for *AR*, showing very compact round spheric structures without any lumen compared with controls without NB treatment (Figures 2B and 2D). This is in agreement with the literature, since organoids that are not stimulated for the androgen pathway show a compact phenotype.[24] By evaluating the distribution of the organoid sizes in the presence or absence of anti-ARgRNA NBs, we indeed confirmed a significant shift toward smaller and more compact organoids (Figure S2). Indeed, a cystic organoid phenotype is dependent on the stimulation of prostate luminal cells by DHT. In addition, it was already demonstrated that incubation with anti-GFP NBs did not induce prostate organoid compactness (Figures 1B and S1).

Nine days after the treatment of the organoids with the NBs, we isolated genomic DNA (gDNA) of the bulk organoid population and amplified a 500-bp-long sequence surrounding the genomic loci targeted by gRNA-AR_1 and gRNA-AR_2 using the AR_ctrl_fw and AR_ctrl_rv primers. Then, these PCR products were subjected to Sanger sequencing. Analysis of the resulting sequences by ICE confirmed that NBs incorporating only gRNA-AR_1 resulted in 12% INDELs, while gRNA-AR_2-containing NBs resulted in 27% INDELs. When the two gRNAs AR_1 and AR_2 were combined in the same NBs, we reached 23% INDELs as shown by a representative ICE analysis, which was confirmed by DECODR analysis (Figure 2C). Confocal microscopic acquisitions of the *AR* KO organoids showed absence of a lumen in the center of the organoid (Figure 2D). Labeling of AR with an anti-AR antibody also confirmed the absence of the AR protein in the compact *AR* KO organoids. Moreover, upon quantification, 20% of the organoids were devoid of AR expression upon treatment with AR2-targeted NBs, showing that a full KO was obtained (Figure 2D).

We also evaluated here the level of toxicity induced by treatment of the organoids with NBs targeting the *AR* gene (Figure 2E) by counting the number of outgrowing organoids 9 days after the treatment with or without NBs. The *AR*-targeted NBs did not significantly affect survival of the cells or their development into organoids, although the *AR* KO resulted in a strong change in phenotype. Clonogenicity is a major asset of the organoid model. Indeed, for prostate organoids, each reseeded progenitor cell will reform a new organoid. The organoid will then have the genetic identity of the initial KO cell. To confirm the efficiency of organoid KO line generation with NBs, we picked 5–10 organoids per condition. For each of these organoid clones, the *AR* locus targeted for gene editing was PCR amplified individually and evaluated for *AR* KO using ICE analysis. For the NBs containing gRNA AR_1, 3 out of 10 organoid lines generated were KO for *AR*, which results in a level of 30% of *AR* KO organoids. For the NBs containing gRNA AR_2, one out of five organoids picked and amplified were KO for *AR*, indicating 20% *AR* KO efficiency

Figure 2. NBs enable efficient generation of KO organoids from mouse prostate organoids

(A) Stepwise procedure and time line for NB-mediated gene KO in organoid cell lines. (B) Bright-field images of mouse prostate organoids at 9 days after treatment with NBs targeting the AR. Two different sgRNAs (AR_1 and AR_2) were used to knock out AR, either alone or in combination. Controls are organoid cells without NB treatment (WT). Scale bar, 200 μm. Representative of n = 3. (C) Bulk gDNA sequencing analysis of organoids treated with AR-targeted NBs. Sanger sequencing was performed of the 557 bp PCR surrounding the AR target loci and was subjected to ICE analysis, which revealed on-target INDEL frequencies at gRNA AR1 or AR2 target loci. Sequence decomposition of INDEL events is shown and is summarized in a histogram (means ± SD, n = 3, technical replicates). (D) Immunofluorescence images of WT and AR KO mouse prostate organoids. Stainings were performed for the basal marker CK5 (cyan), luminal marker CK8 (red), and AR (green). Nuclei were stained with DAPI (blue). Scale bar, 50 μm. The number of organoids positive for AR staining were quantified (means ± SD, n = 3), ***p< 0.001. (E) The toxicity in organoids was evaluated 9 days after treatment by counting the number of organoids treated or not with NBs targeting AR using a counting cell (means ± SD, n = 3, biological replicates, one-way ANOVA, Tukey's multiple comparisons test; ns, not significant). (F) Individual organoid clones were picked for NBs carrying the two different gRNAs (AR_1 or AR_2). Sanger sequencing was performed of the 557 bp PCR surrounding the AR target loci and was subjected to ICE analysis which revealed on-target INDEL frequencies at gRNA AR1 or AR2 target loci for each organoid clone.

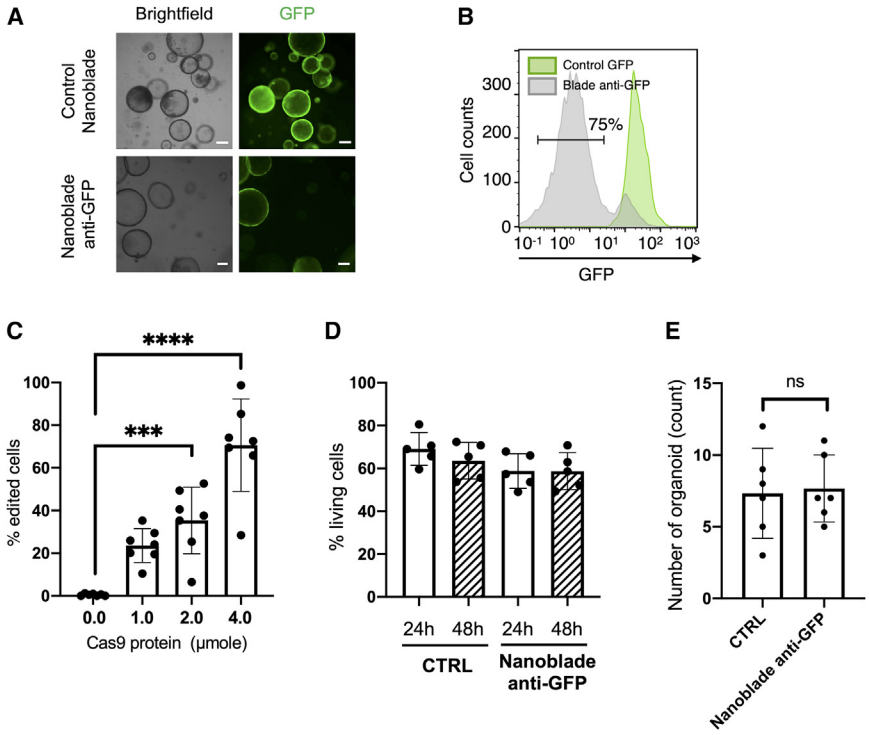

Figure 3. Efficient NB-induced KO in mouse colon organoids

(A) Representative bright-field images of mouse colon organoids 9 days after treatment or not with anti-GFP NBs. Scale bar, 200 µm. (B) Flow cytometry analysis of eGFP-expressing organoids treated or not with NBs targeting the eGFP coding sequence. (C) Flow cytometry analysis of eGFP-expressing organoids treated with different quantities of anti-GFP NBs; the percent of GFP− cells indicates the percent of editing cells (means ± SD, n = 6, biological replicates, one-way ANOVA, Tukey's multiple comparisons test; ***p < 0.001, ****p < 0.0001). (D) FACS analysis for living colon organoid cells (DAPI+) 24 or 48 h after incubation or not with NBs (means ± SD, n = 6, biological replicates, t test, Mann-Whitney test, non-parametric; ns, not significant). (E) Toxicity of NBs in organoids was evaluated 9 days after treatment by counting the number of organoids treated or not with NBs using a counting cell (means ± SD, n = 6, biological replicates, t test, Mann-Whitney test, non-parametric; ns, not significant).

(Figure 2F). Moreover, for the gene-edited clones we confirmed that the entire organoid showed the same INDEL (Figure S3).

Concluding, we obtained high-level KO for AR in prostate organoids and this was without induction of cellular toxicity.

NBs allow efficient gene editing in mouse colon organoids

Colon organoids were one of the first organoid models to have been developed.[29] They are also cultured in Matrigel. The culture medium is slightly different in composition compared with that used for culture of mouse prostate organoids, as described in materials and methods. The NB-mediated editing efficiency and toxicity might be different according to the type of organoid; therefore, both parameters were evaluated in colon organoids.

As described above for prostate organoids, NB gene-editing efficiency in colon organoids was initially tested by knocking out eGFP in colon organoids expressing eGFP. Similar to the prostate organoids, we established a mouse colon organoid cell line expressing eGFP. We incubated the dissociated colon organoid cells with anti-GFP NBs for only 3 h and grew them into organoids. Fluorescence microscopy demonstrated a strong reduction in eGFP+ organoids (Figure 3A). The bulk population of dissociated organoids was quantified by FACS for NB-mediated loss of eGFP (Figure 3B). We obtained with the colon organoids similar levels of KO as for the prostate organoids. Indeed, with the maximum dose of anti-GFP NBs we achieved on average a gene-editing efficiency of 70% for the colon organoid cells (Figure 3C). Short-term toxicity was evaluated by DAPI staining 24 and 48 h after NB incubation or not. NBs did not increase cell death of colon organoid cells (Figure 3D). Equivalent to prostate organoids, after treatment of dissociated colon organoid cells with the maximum dose of NBs tested (4 µmol of Cas9 protein) no significant toxicity was detected since the number of cells developing into organoids was equivalent in the presence or absence of NBs (Figure 3E). Moreover, the size distribution of the organoids was not changed after anti-GFP NBs incubation versus no incubation with NBs (Figure S4A).

Overall, this first evaluation of NB-mediated gene editing in mouse colon-derived organoids shows a very high efficiency of genome editing with low toxicity, equivalent to what we observed for prostate organoids.

NBs allow efficient CFTR gene KO in mouse colon organoids

As mentioned previously, CFTR is an anion channel activated by cAMP-dependent phosphorylation.[30] Previous studies have shown that CFTR is responsible for fluid secretion into the lumen and swelling of organoids.[10,15,23]

Here, we used the same experimental approach for *AR* KO in prostate organoids for colon organoids (Figure 2A). We designed two gRNAs targeting the mouse *CFTR* gene (exon 14/exon 27) and treated the colon organoids for 3 h with NBs carrying the CFTR_1, CFTR_2, or CFTR_1 and CFTR_2 gRNAs (Figure 4A).

Nine days after the treatment of the organoid cells with the NBs and their outgrowth in colon organoid medium, we isolated gDNA of the bulk organoid population (Figure 4B). We amplified a 625-bp genomic fragment around the loci targeted by the CFTR_1 sgRNA

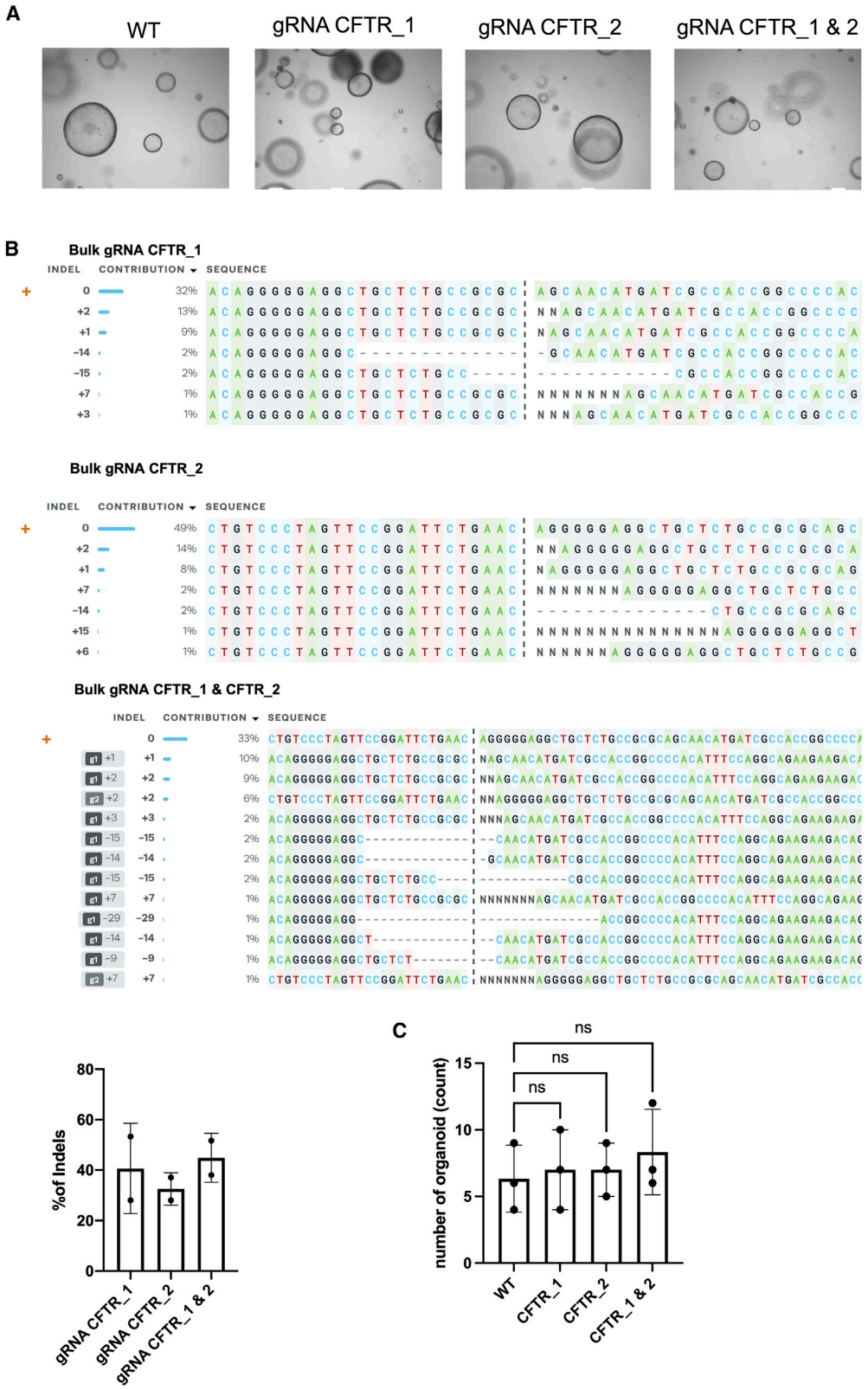

(legend on next page)

or CFTR_2 sgRNA. The INDEL analysis performed by ICE software showed an average INDEL frequency of 40% for CFTR_1 sgRNA and 32% for CFTR_2 sgRNA. The percentage of INDELs reached 44% when both guide RNAs were provided by the same NB preparation.

Toxicity was also evaluated by counting the number of organoids that developed 9 days after treatment in the presence or absence of the NBs (Figure 4C). Here, again, the NBs did not induce toxicity compared with the control conditions. Moreover, the size distribution of the organoids was not significantly changed after anti-CFTR NB incubation versus no incubation with NBs (Figure S4B).

NB-mediated gene editing was thus also highly efficient for mouse colon organoids underlining the ease and versatility of NBs for gene editing and KO generation in the mouse organoid model.

NBs do not induce INDELs at the analyzed off-target sites in murine organoids

Another advantage of the NBs is that we provide Cas9 as a protein. The CRISPR-Cas9 gRNA complexes, so-called RNPs, contained in the VLPs are only transiently present once delivered into the targeted cell.[26] The fact that Cas9 is present in the cell for a limited time should decrease the number of cuts in off-target sites, as shown previously.[25] Using the Cas-OFFinder software, we predicted potential off-target sites for each of our sgRNAs (Tables S1 and S2). We included in our analysis only the off-target sites containing a protospacer adjacent motif (PAM). We assessed two off-target sites for the AR_1 sgRNA with three mismatches since no off-target sites with one or two mismatches were identified by Cas-OFFinder (Figure 5A; Table S1). One was located on chromosome 9 and the other one on chromosome 13. We designed PCR primers (see materials and methods) to amplify by PCR a 602-bp region around the chromosome 9 off-target site, and a 622-bp fragment including the potential chromosome 13 off-target site. For the AR_2 sgRNA off-target no sequences with one, two, or three mismatches were predicted and only off-target sites with four mismatches were identified compared with the target locus, of which we randomly choose two for off-target INDEL analysis (Figure 5A; Table S2). We amplified by PCR the off-target regions in the gDNA isolated from the organoid bulk treated with either AR_1 or AR_2 sgRNA and Sanger sequenced the PCR products. Analysis for INDELs by ICE showed that no gene editing was detected in the off-target sites analyzed (Figure 5B). This was confirmed by DECODR analysis.

We also predicted the potential off-target sites for the sgRNAs CFTR_1 and CFTR_2 using the open access program Cas-OFFinder (Tables S3 and S4; no more than three mismatches are listed). We proceeded as for *AR* gRNA off-targets and, under these experimental conditions, no off-target gene editing was detected for the four different *CFTR* off-target positions analyzed (Figures 5C and 5D).

NBs allow efficient gene editing in human colon organoids

Human organoids such as intestinal or prostate organoids subjected to lentiviral transduction or electroporation to introduce the CRISPR-Cas9 machinery result in more cellular toxicity than their murine counterparts. Since the NB technology performed gene editing in murine organoids without a significant toxic side effect, we wanted to evaluate the efficacy of NB-mediated gene editing in human organoids. Firstly, as a proof of principle we generated GFP-expressing human prostate organoids (45% GFP+), which we exposed to several doses of GFP-targeted NBs for 5 h. Nine days after organoid culture, we detected 50% loss of GFP in the bulk population of organoids as detected by FACS (Figure S5) corresponding to 50% gene editing at the highest doses of NBs (4 μmol of Cas9 protein). Importantly, no difference in human prostate organoid frequency and structure as demonstrated by immunofluorescence staining was detected with or without NB incubation (Figure S5D). Subsequently, we generated eGFP-expressing human rectal organoids by short exposure to an LV-expressing eGFP. Without sorting we exposed the human organoid cells (30% GFP+) to anti-GFP NBs (4 μmol of Cas9 protein) for only 10 min to avoid toxicity on organoid growth since longer incubation to viral particles was toxic, as shown previously.[31] In parallel, we treated dissociated organoid cells by electroporation with a Cas9-encoding plasmid and the same anti-GFP gRNA-encoding plasmid used for the NB production since this is still the main approach in the organoid field. The cells were then seeded in Matrigel. Without any prior enrichment for edited cells, the cells were grown into organoids for 14 days. The bulk population of dissociated organoids was quantified by FACS for NB-mediated loss of eGFP (Figure 6A). Over 50% of the GFP+ organoids lost eGFP expression upon NB incubation, indicating 50% gene editing in these human intestinal organoids. In contrast, electroporation of the Cas9/anti-GFP gRNA-encoding plasmids resulted only in 15% of loss of GFP+ organoid cells (Figure 6A, middle panel). Moreover, at 72 h post treatment no decrease in organoid cell survival was detected for the NBs and their organoid structure was intact (Figure 6A, right panel, and Figure S6). In contrast, electroporation caused significant cell death, reaching 50% for the intestinal organoids. Of note, for breast-derived organoids electroporation was even more toxic (70% cell death; Figure S7). Subsequently, we designed a gRNA against human *CFTR*, which we first validated in the context of NBs

Figure 4. NBs allow efficient KO of CFTR in mouse colon organoids

(A) Representative bright-field images of mouse prostate organoids 9 days after treatment with NBs targeting CFTR. Two different sgRNAs were used to knock out CFTR, which were employed alone or in combination. Controls are organoid cells without NB treatment (WT). (B) Bulk gDNA sequencing analysis of organoids treated with NBs targeting CFTR. Sanger sequencing was performed of PCR bands including the CFTR target loci and subjected to ICE analysis, which revealed on-target INDEL frequencies at gRNA CFTR_1 or CFTR_2 target loci. Sequence decomposition of INDEL events is shown and are summarized in a histogram (means ± SD, n = 2, biological replicates). (C) Toxicity of NBs in organoids was evaluated 9 days after treatment by counting the number of organoids treated or not with NBs using a counting cell (means ± SD, n = 3, biological replicates, one-way ANOVA, Tukey's multiple comparisons test; ns, not significant).

A

Selected off-target sites for CRISPR/Cas9_gRNA AR_1 & gRNA AR_2

crRNA	gDNA	Chromosome	Direction	Mismatches
ATGTACGCGTCGCTCCTGGGNGG	ATGTACaCtTtGCTCCTGGGTGG	chr9	+	3
TTCAAGGGAGGTTACGCCAANGG	TaCAAGGGAGGTTACtCaAcAGG	chr8	+	4
TTCAAGGGAGGTTACGCCAANGG	TTCAAGGaAGGTTcCctCAATGG	chr15	-	4

B

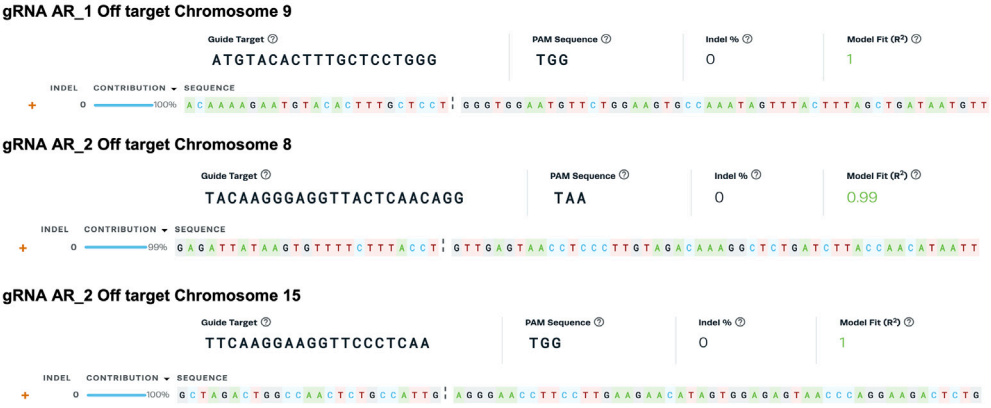

C

Selected off-target sites for CRISPR/Cas9_gRNA CFTR_1 & gRNA CFTR_2

crRNA	gDNA	Chromosome	Direction	Mismatches
GTGGCGATCATGTTGCTGCGNGG	GTGGCcATCATGTTGgTGCtGGG	chr14	-	3
GTGGCGATCATGTTGCTGCGNGG	GTGGCctTCATGTTGCTGCaCGG	chr13	-	3
AGTTCCGGATTCTGAACAGGNGG	AGTTtCtGtTTCTGAACAGGTGG	chr8	+	3
AGTTCCGGATTCTGAACAGGNGG	AGTTCtGGAcTCTGAgCAGGGGG	chr2	+	3

D

Figure 5. Off-target genotoxicity was not detected upon NB-mediated KO of genes in organoids

(A) Cas-OFFinder algorithm was used to identify potential off-target sites for the sgRNAs AR1 and AR2, of which three are listed (see Table S1). (B) Sanger sequencing of sgRNAs AR1 and AR2 potential off-target loci subjected to ICE analysis revealed no off-target DSBs. (C) Cas-OFFinder algorithm was used to search for potential off-target sites for the sgRNAs CFTR_1 and CFTR_2, of which four are listed (see Table S1). (D) Sanger sequencing of sgRNAs CFTR_1 and CFTR_2 potential off-target loci subjected to ICE analysis revealed no off-target DSBs.

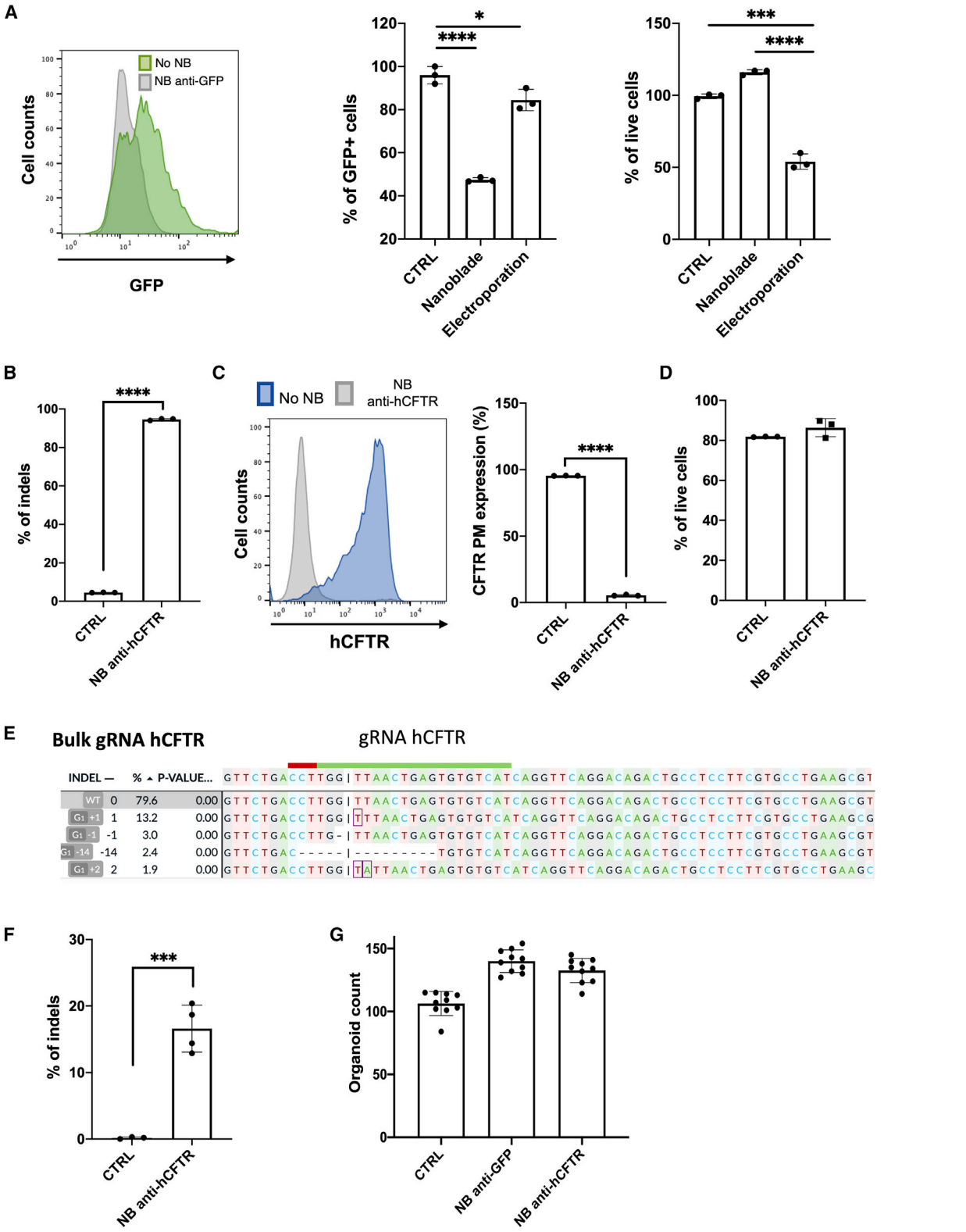

(legend on next page)

(anti-hCFTR NB) in HEK293T-CFTR-HAtag cells. These HEK293T overexpress hCFTR due to an integrated *CFTR* cDNA copy tagged by an extracellular 3HA-Tag for detection by flow cytometry.[32] After the treatment with the NBs, gDNA of the bulk HEK293T cells was isolated and the sequence surrounding the genomic locus targeted by the hCFTR sgRNA was amplified using the *hCFTR* Fw and Rv primers (Table S5). These PCR products were then subjected to Sanger sequencing. Analysis of the resulting sequences by ICE confirmed that anti-hCFTR NBs resulted in over 90% INDELs (Figure 6B). The high-level KO of *hCFTR* in HEK293T was confirmed by almost complete disappearance of *hCFTR*-HA-tagged surface expression (Figure 6C). As detected previously, no cell death was induced by the NBs in 293T cells (Figure 6D).[26]

Finally, the rectal organoids were, upon dissociation, incubated solely for 10 min with these validated anti-hCFTR NBs. We amplified a genomic fragment around the loci targeted by the hCFTR sgRNA. The INDEL analysis performed by DECODR software showed an INDEL frequency up to 20% for the *hCFTR* genomic target site (Figures 6E and 6F). Finally, no apparent toxicity was detected since the number of cells developing into human organoids was similar in the absence or presence of anti-GFP or anti-hCFTR NBs (Figure 6G).

Concluding, even in human organoids NBs allow high-level gene editing without toxicity.

DISCUSSION

Here, we have shown an effective delivery methodology for the CRISPR-Cas9 system called "nanoblades," which permitted to obtain high levels of gene editing (20%–80%) in human and mouse organoids without the requirement for enrichment via drug selection or fluorescent reporter isolation.[33] These are levels of gene editing that are otherwise exclusively achieved in iPSC-derived organoids.[34] Brain organoids, for example, are solely derived from iPSCs and since gene editing is performed at the level of the iPSCs, which is highly efficient, deleting genes or introducing genes (e.g., oncogenes) can be performed with ease.[35] In comparison, ASC-derived organoids showed very low levels of gene editing using the same gene-editing tools.

NBs, in contrast to other gene-editing techniques, have major advantages: they incorporate the Cas9 associated with gRNA cargo as RNPs, which they deliver via pseudotyped VLPs. This allows, in contrast to LV delivery,[36] a transient expression of Cas9. Until very recently,[22] most studies performing gene editing in organoids used plasmid DNA to introduce the gene-editing machinery. For example, two studies published in 2013 and 2015 introduced plasmid DNA by liposome transfection into adult stem cells.[10,37] The study published in 2013, which described the use of the CRISPR-Cas9 system to correct the CFTR mutations in organoids derived from cystic fibrosis patients, showed low levels of gene editing.[10] The same research team reported the use of CRISPR-Cas9 to induce sequential cancer. mutations in cultured human intestinal stem cells; also in this context, they achieved low levels of gene editing (<1%). In these two cases, these low levels of gene editing might depend on the delivery method.[37] Indeed, a study published in 2015[11] showed higher levels of gene editing. In this case the introduction of DNA plasmid into organoid cells was performed by electroporation. This change of delivery method allowed a 4-fold increase in efficiency. However, the levels of gene editing still did not exceed 1%.[38]

To counteract these low efficiency levels, which makes the use of CRISPR-Cas9 in organoids time-consuming and inefficient, several groups developed more efficient reporter gene knockin techniques.[13,22,39] The insertion of a fluorescent cassette into the Cas9-induced DSB allows for easier identification of the edited organoids. Despite the advantage of this approach, it should be noted that the addition of a knockin cassette adds an additional difficulty because a donor template sequence needs to be co-introduced together with the gene-editing system into the cell. Furthermore, the knockin levels achieved by electroporating plasmid DNA remained below 5%.[13] Alternatively, an NHEJ strategy relying on the piggybac-transposase system to integrate hygromycin/GFP was used to screen for fluorescence or drug resistance.[13]

Viruses have already been used for a long time to genetically manipulate cells. The efficiency of the best performing viral vectors such as LVs can reach 100% transduction of the targeted cells.[40] In this study, as proof of principle, we evaluated for the first time VLPs

Figure 6. Efficient NB-induced KO in human intestinal organoids

(A) Human rectal eGFP-expressing organoids 14 days after treatment or not with anti-GFP NBs or electroporation with Cas9 and anti-GFP gRNA encoding plasmid. Flow cytometry analysis of percent eGFP-expressing organoid cells (left panels, representative of n = 3). The viability (right panel) upon treatment with anti-GFP NBs or electroporation of Cas9 and anti-GFP gRNA encoding plasmids is shown after 72 h (means ± SD, n = 3, biological replicates, t test, Mann-Whitney test, non-parametric; ****$p < 0.0001$, ***$p < 0.001$, *$p < 0.05$). (B and C) Validation of anti-hCFTR NBs in HEK293T cells. (B) One sgRNA was used for KO of human CFTR in HEK293T cells. Bulk gDNA sequencing analysis of the cells treated with NBs targeting hCFTR. Sanger sequencing was performed of the PCR band including the hCFTR target locus and was subjected to DECODR analysis, which revealed on-target INDEL frequencies at the gRNA CFTR target locus (means ± SD, n = 3, biological replicates, t test, Mann-Whitney test, non-parametric; ****$p < 0.0001$). (C) Detection of hCFTR plasma membrane (PM) expression by FACS analysis for HEK293T cells, overexpressing 3HA-CFTR treated with anti-hCFTR NBs or control NBs (means ± SD, n = 3, biological replicates, t test, Mann-Whitney test, non-parametric; ****$p < 0.0001$). (D) Toxicity of NBs in HEK293T cells by DAPI staining at 48 h after NB incubation (means ± SD, n = 3, biological replicates, unpaired t test, not significant). (E) Bulk gDNA sequencing analysis of human rectal organoids treated with NBs targeting hCFTR. Sanger sequencing was performed of the PCR band including the CFTR target locus and was subjected to DECODR analysis which revealed on-target INDEL frequencies at the gRNA hCFTR target locus. Sequence decomposition of INDEL events is shown (upper panel) and is summarized in the histogram (F) (means ± SD n = 4, technical replicates, t test, Mann-Whitney test, non-parametric; ***$p < 0.001$). (G) Toxicity of NBs in organoids was evaluated 14 days after treatment by counting the number of organoids treated or not with NBs (means ± SD, n = 10, technical replicates). CTRL, no NBs.

incorporating CRISPR-Cas9 anti-GFP gRNA complexes called NBs for eGFP KO in eGFP-expressing human and murine organoids. We reached up to 80% of edited cells, underlining that this technique is more efficient than any other methods inducing a gene KO in organoids.

A crucial concern for any Cas9-mediated gene-editing technology is the possibility of off-target editing. When Cas9 cDNA is introduced into cells by a plasmid, it results in a sustained presence of Cas9 protein in the cells and this increases the risk of INDELs at off-target sites. A recent study reported the nucleofection of RNPs to edit organoids.[22,41] This approach had two advantages. First, in a detailed comparison of the different types of cargo to deliver Cas9, RNPs coupled to single-strand gRNAs were more efficient than plasmid DNA encoding Cas9 for editing cells. The second advantage is the reduction of off-target effects. Indeed, by providing Cas9 as a protein, its presence in the cell is considerably reduced. Therefore, the off-target effects are decreased.[42] As expected, when we provided Cas9 RNPs via NBs none of the NBs induced non-specific cleavage at the analyzed off-target genomic sequences that were evaluated by Sanger sequencing and ICE and DECODR analysis. Of note, the repair of a DSB induced by CRISPR-Cas9 is error-prone and can give unwanted mutations at the target as well as the off-target genomic loci. A way to avoid these unwanted editing events in organoids might be to use CRISPR-based prime editing[15] or base editing, especially since Liu and co-workers recently showed that they were able to develop NB-like VLPs harboring the base editing machinery and achieve efficient base editing.[43]

Another advantage of the NBs is the absence of toxicity for the treated organoid cells. Indeed, electroporation remains harsh for the organoid cells as shown also by us for the human colon organoids, which are very fragile. Mammalian cells are sensitive to the voltage and the time of application of the current, even when electroporating RNPs.[42] Importantly, this means that one can easily perform a second round of incubation with the same NBs to increase the KO levels in the organoids without toxicity.

In this study, we report the generation of an *AR* KO organoid prostate line. As shown previously, luminal cell KO for *AR* failed to achieve terminal differentiation.[44] In addition, it was reported that the swelling of luminal organoids is directly dependent on the stimulation of the androgen pathway.[24] In accordance, the organoid KO for *AR* that we generated here induced a compact phenotype. The lumen formed by fluid secretion from the luminal cells did not occur when the cells were KO for *AR*. It would be interesting to understand whether the absence of lumen is indeed due to impaired terminal differentiation of luminal cells. Further studies using single-cell RNA sequencing, for example, would allow to fully understand this observation.

We have also demonstrated for the KO of two different genes (AR and CFTR) that we can multiplex the NBs with two gRNA directed against different target sequences of the same gene. Previously, it was demonstrated that NBs can be loaded with multiple gRNAs, even with up to four different gRNAs.[25,26] Therefore, NBs might pave the way to study tumorigenesis in gastrointestinal malignancies[45] and beyond. It is well known that cancers develop through sequential accumulation of oncogenic mutations. NBs will allow generation of KOs in multiple genes simultaneously to study their role in cancer development, as performed before by fluorescent molecule knockin for ovarian cancer.[46] However, some complex organoids require strong reorganization of multiple cell types and layers, which cannot be simply dissociated into single cells that will, upon reseeding, give rise again to these complex structures. So further evaluation is needed for this kind of organoids.

Overall, NBs represent a versatile and highly efficient tool to edit human and murine organoids *in vitro*. They allow to obtain rapid and efficient gene KO in several organoid models with gene-editing levels that outperform other currently used techniques, while requiring only transient expression of the gene-editing machinery. Of utmost importance, efficient gene editing in organoids is accompanied by low cellular toxicity and low off-target effects, which is due to the transient RNP delivery by this system. Finally, the experimental strategy is fast since it allows us to generate organoid lines in 4–6 weeks with high efficiency. In addition, NBs offer the possibility to efficiently generate high-level editing in organoids without the need to use reporters encoding knockin cassettes or a drug selection method. Therefore, NBs might allow studies in tissue differentiation, cancer development, and drug screening, as well as preclinical evaluation of correction by gene therapy in organoids and possibly will allow to facilitate multiple other gene-editing applications using organoids.

MATERIALS AND METHODS

Organoid culture

Mouse prostate organoids were generated as described by Drost et al.[5] In brief, the prostates of 7- to 8-week-old male C57BL/6JOlaHsd mice (ENVIGO, Cannat, France) were isolated, and minced in small fragments. Tissue fragments were digested with type II collagenase at 5 mg/mL for 1 h at 37°C and subsequently incubated with 1X TrypLE (Gibco, Waltham, MA) for 15 min at 37°C. Cells were washed between each step with 15 mL of advanced complete DMEM/F12 (adDMEM/F12 containing penicillin/streptomycin, 10 mM HEPES, and 2 mM GlutaMAX [(100× diluted]) (Thermo Fisher Scientific, Waltham, MA). Then cells were passed through a 70-μm cell strainer (Thermo Fisher Scientific) to remove large cell debris. The cells were then labeled with CD49f-APC (Thermo Fisher Scientific, clone GoH3; RRID: AB_891474) and CD24-PE (BioLegend, clone M1/69, RRID: AB_493485) conjugated antibodies and were sorted for the CD49f+ CD24− cells by flow cytometry (BD FACSAria Cell Sorter). The isolated cells were then washed with complete adDMEM/F12 and, after centrifugation at 200 × *g* for 5 min, the cell pellet was resuspended in growth factor reduced phenol red-free Matrigel (Corning, NY) at a concentration of 200 cells per μL Matrigel. Mouse prostate organoids were maintained in complete adDMEM/F12 supplemented with 50× diluted B27 (Life Technologies, Carlsbad, CA), 1.25 mM N-acetyl-L-cysteine (Sigma-Aldrich, St. Louis, MO), 50 ng/mL EGF (PeproTech, Cranbury, NJ), 200 nM A83-01 (Tocris Bioscience, Bristol, UK), 1% Noggin conditioned medium, 10%

R-spondin 1 conditioned medium, 1 nM DHT (Sigma-Aldrich), and 10 μM Y-27632 dihydrochloride (PeproTech). Culture medium was replenished every 2 days.

Mouse colon organoids were established from colons of male C57BL/6JOlaHsd mice (ENVIGO) and maintained in complete adDMEM/F12 supplemented with 50× diluted B27 (Life Technologies), 100× diluted N2 (Life Technologies), 1 mM N-acetyl-L-cysteine (Sigma-Aldrich), 50 ng/mL EGF (PeproTech), 1% Noggin conditioned medium, 20% R-spondin 1 conditioned medium, 50% Wnt3a conditioned medium, and 10 μM Y-27632 dihydrochloride (PeproTech). Culture medium was replenished every 2 days.

For passage of the organoid cultures, each drop of Matrigel containing the organoids was resuspended in 1 mL of ice-cold complete adDMEM/F12, which was centrifuged for 5 min at 200 × *g* at 4°C. Prostate and colon organoids were then incubated in TrypLE for 5 and 3 min, respectively, at 37°C and mechanically dissociated by pipetting up and down with a P10/P1000 pipet tip. Cells were then washed with complete adDMEM/F12 and centrifuged. Cells were seeded back in Matrigel at a concentration of 100 cells/μL. The appropriate medium was added to the cells and replenished every 2 days. Organoids were passaged every 7–10 days.

Human rectal organoids were generated and cultured as described previously.[47] Informed consent was obtained before biopsy collection, in accordance with the ethical committee of UZ Leuven (S56329). Human rectal organoids were generated form rectum biopsies of PwCF as described previously and biobanked after successful culture.[47] Organoids from the biobank were thawed and cultured for evaluation in this study. Human prostate organoids were a kind gift from Yu Chen (Memorial Sloan, New York) They were maintained in complete AdDMEM/F12 supplemented with 50× diluted B27 (Life Technologies), 10 mM Nicotinamide (Sigma-Aldrich), 1.25 mM N-acetyl-L-cysteine (Sigma-Aldrich), 10 μM SB202190 (Sigma-Aldrich), 5 ng/mL EGF (PeproTech), 5 ng/mL FGF2 (PeproTech), 10 ng/mL FGF10 (PeproTech), 500 nM A83-01 (Tocris Bioscience), 1 μM prostaglandin E2 (Tocris Bioscience), 1% Noggin conditioned medium, 10% R-spondin 1 conditioned medium, 1 nM DHT (Sigma-Aldrich), and 10 μM Y-27632 dihydrochloride (PeproTech). Culture medium was replenished every 2 days.

Plasmids

All the plasmids (Gagpol MLV, GagMLV-Cas9, VSV-G) and gRNA-expressing plasmids to produce the NBs were described previously[25,26] and are available at Addgene (https://www.addgene.org). SP-dCas9-VPR was a gift from George Church (Addgene, plasmid no. 63798). Lenti CRISPR was a gift from F. Zhang (Addgene, plasmid no. 49535). The GagMLV-CAS9 fusion was constructed by sequential insertions of PCR-amplified fragments in a eukaryotic expression plasmid harboring the human cytomegalovirus (CMV) early promoter, the rabbit β-globin intron, and polyadenylation signals. The MA-CA-NC sequence from Friend murine leukemia virus (accession no. M93134) was fused to the MA/p12 protease-cleavage site (9 aa) and the Flag-nls-spCas9 amplified from pLenti CRISPR. The BaEVRless envelope glycoproteins were described previously[28] and can be obtained under material and transfer agreement from the corresponding author (E.V.). The BaEVRless envelope glycoprotein is from the baboon endogenous retrovirus and its R-peptide was removed to improve LV pseudotyping as described. Both envelope glycoproteins (VSV-G and BAEV) were expressed in the phCMV-G expression plasmid.[48] The HIV-SFFV-eGFP vector and the HIV CMV-eGFP LV encoding plasmids to produce the GFP murine and human organoid cell line were described previously.[31,49]

Cell lines

HEK293T kidney cell line (ATCC CRL-3216) was grown in DMEM (Life Technology, Paris, France) medium with 10% FCS and 50 μg/mL of penicillin/streptomycin (Invitrogen). A HEK293T cell line was generated previously to overexpress human CFTR due to an integrated *CFTR* cDNA copy tagged by an extracellular 3HA-Tag,[32] called here 293T-CFTR-HATag.

Lentiviral production

LVs encoding the reporter gene eGFP were produced as described previously.[28] In brief, self-inactivating (SIN) HIV-1-derived vectors were generated by transfection of 2×10^6 293T cells per 10-cm culture plate in DMEM/10% FCS. Co-transfection by Ca_2-PO_4 precipitation was performed with the Gag-Pol packaging construct 8.91 (8.6 μg) and the SIN HIV-1-derived vector coding for the GFP reporter under the control of an SFFV promoter (SIN-HIVSFFVGFP; 8.6 μg). For display of RDTR, BaEVTR, and BaEVRLess glycoproteins on LVs, 7 μg of plasmid coding for these glycoproteins were co-transfected. For VSV-G-LV production, 3 μg of VSV-G encoding plasmid were transfected. At 16 h post-transduction, the supernatant was replaced by Opti-MEM medium supplemented with HEPES (Invitrogen, Carlsbad, Californie, États-Unis). Viral supernatant was harvested 48 h post-transfection and filtered through a 0.45-μm pore-sized membrane. Low-speed centrifugation of the vectors was performed by overnight centrifugation at 3,000 × *g* at 4°C. Concentrated vectors are aliquoted and stored at −80°C. Titration was performed by adding serial dilutions of vector to 293T cells and the MOIs were expressed using 293T titers.

Vector copy number detection per cell

Estimation of the mean vector copy number per transduced cell was obtained by qPCR performed on human CB $CD34^+$ cells 10 days after transduction. gDNA was prepared using NucleoSpin Tissue XS kits (Macherey Nagel, Hoerdt, France). Average vector copy numbers were determined by qPCR with primers amplifying the packaging signal (primers: fwd: TGT GTG CCC GTC TGT TGT GT; rev: GAG TCC TGC GTC GAG AGA GC; probe: CAG TGG CGC CCG AAC AGG GA) after normalization for endogenous b-actin genes (primers: fwd: TCC GTG TGG ATC GGC GGC TCC; rev: CTG CTT GCT GAT CCA CAT CTG; probe: CCT GGC CTC GCT GTC CAC CTT CCA). Results were compared with those obtained after serial dilutions of gDNA from a cell line containing one copy of the integrated LV per haploid genome.

sgRNA design

The sgRNAs of the different targeted genes were cloned into the gRNA-expressing plasmid using the BsmBI restriction site.[25] The sequences of the sgRNA are as follows.

GFP_B182	5′-CGAGGAGCTGTTCACCGGGG-3′
Ms_AR_1	5′-ATGTACGCGTCGCTCCTGGG-3′
Ms_AR_2	5′-TTCAAGGGAGGTTACGCCAA-3′
Ms_CFTR_1	5′-GTGGCGATCATGTTGCTGCG-3′
Ms_CFTR_2	5′-AGTTCCGGATTCTGAACAGG-3′
Hu_CFTR	5′-GGAGAACTGGAGCCTTCAGA-3′

Production of NBs

NBs were produced in human HEK293T kidney cell line (ATCC CRL-3216). Cells (5×10^6) were seeded per 10-cm culture plate 24 h before transfection. To produce NBs, plasmids coding for MLVGagPol (3 μg), GagCas9 (3 μg), BaEVRless (2 μg), VSVG (2 μg), and gRNA expression plasmid (6 μg) were co-transfected with transfection reagent at a 2.6/1 ratio of polyethylenimine (Polysciences, Warrington, PA) (μg)/total DNA (μg). The medium was replaced 24 h after transfection by 6 mL of OptiMEM (Life Technologies) supplemented with penicillin/streptomycin (1%) and HEPES (1%). The next day, NB-containing medium was clarified by centrifugation (2,000 rpm for 5 min) and filtered through a 0.45-μm pore-sized filter before centrifugation overnight (3,000 × *g* for 16 h at 4°C). The supernatant was carefully removed by aspiration to obtain 100–150× concentration of the NB preparation. NBs can be stored at −80°C.

Cas9 quantification in the NBs by ELISA

Recombinant Cas9 (New England Biolabs) was used to generate a standard curve (20 μM, 6 serial dilutions of 1/2), while the NB supernatants were diluted 1/200 and 1/400. The dilutions were performed in coating buffer (1% Triton) and were then coated onto 96-well plates by incubation overnight at 4°C. The following day, the wells were incubated with washing buffer (PBS/0.05% Tween) and blocked with PBS/0.05%Tween/3%BSA (Sigma). Subsequently, the wells were washed and the primary anti-Cas9 antibody (Cas9-7A9-3A3, 14697P; Cell Signaling Technology) was added at 1/1,000 dilution in PBS/3%BSA, and incubated at room temperature (RT) for 1 h, while shaking. Before and after 1 h incubation with a secondary anti-mouse HRP (F6009-X639F South Biotech) diluted 1/10,000 in PBS/3%BSA, a wash step was performed. Finally, the mixed TMB substrate solution containing HRP substrate was added for 20 min (Bethyl Laboratories, Montgomery, TX). Stop reaction was added in each well and protein was measured at 450 nm in a Multiskan FC (Thermo Scientific).

NB transduction procedure

Murine organoids

Murine prostate and colon organoids from passages 5–10 were used for the gene-editing experiments; they were resuspended in ice-cold complete adDMEMF/12, then centrifuged at 200 × *g* for 5 min at 4°C. Once the supernatant was aspirated, 1× TrypLE was added to the tube and incubated for 5 min at 37° C while pipetting up and down to dissociate the organoids.

For mouse prostate and colon organoids, after washing the cells with complete adDMEMF/12, 1×10^4 cells were distributed in a 96-well plate in 100 μL of complete adDMEMF/12 with 10 μM Y-27632, to which NBs (4 μmol of Cas9 protein) were added. The plate was then centrifuged at 200 × *g* for 60 min at RT and incubated for 6 h at 37°C. Colon organoid cells were only incubated with NBs for 3 h. The cells were then collected in a 15-mL tube containing 5 mL of complete adDMEMF/12 and centrifuged at 200 × *g* for 5 min. The supernatant was removed and the cells were resuspended in 100 μL of Matrigel and drops of 40 μL were deposited in 24-well plates. After an incubation of 15 min at 37° C, 500 μL of mouse prostate organoid medium was added to each well as described previously. Alternatively, the 96-well plate can be coated with RetroNectin (Clontech/Takara; 12 μg/mL PBS according to the manufacturer's recommendations) overnight at 37°C before seeding the cells and addition of the NBs. Polybrene (6 μg/mL) was added in some conditions, as indicated, to the NBs to enhance the transduction efficiency.

Human organoids

Human intestinal organoids were used at passages 8–10 for the gene-editing experiments; they were trypsinized to single-cell suspension and then human rectal organoids were centrifuged for 5 min at 200 × *g*. The cell pellet was resuspended with 10 μL of NB preparation per 6×10^3 cells (*CFTR* KO experiment) or per 1.4×10^4 cells (eGFP KO experiment) and incubated at RT for only 10 min. The cells loaded with NBs were then resuspended with Matrigel and seeded into a 24-well plate. The plate was incubated 15 min at 37°C. Subsequently, the complete organoid medium,[50] supplemented with rho-kinase inhibitor Y-27632 (10 μM), was added for 3 days to the solidified Matrigel drops. For electroporation, organoids were dissociated to singlets by trypsinizing them. Electroporations were performed using Neon Electroporator 100 μL tips (Thermo Fisher Scientific) with the following parameters: 1,700 V, 1 pulse, 20 ms, and 10,000 cells/μL. Once electroporated, the cells were then resuspended with Matrigel and seeded into a 24-well plate. The plate was incubated 15 min at 37°C. Subsequently, the complete organoid medium,[50] supplemented with rho-kinase inhibitor Y-27632 (10 μM), was added for 3 days to the solidified Matrigel drops, which was replaced and then every other day for 7 days. Organoids were then detached and dissociated for FACS analysis. Human prostate organoids were used at passages 9–11 for gene-editing experiments. They were cultured and treated with NBs in a similar way, but we increased the NB incubation to 5 h.

Establishment of murine and human organoid lines expressing eGFP: we used a LV (plasmid pHIV-SFFV-IRES-eGFP),[51] which contains an eGFP under the control of an SFFV promoter or a LV pHIV-CMV-eGFP with eGFP under the control of the CMV promoter.[31] The transduction procedure is the same as the one used for the NBs. We applied a low MOI of 0.3 to ensure that we obtained only one integrated copy of the eGFP expression

cassette into the genome of the mouse organoids. We then sorted the cells by flow cytometry for eGFP+ cells (BD FACSAria Cell Sorter). We seeded the sorted murine organoid cells in Matrigel at a concentration of 200 cells/μL. Then the corresponding medium was added and replenished every 2 days.

Flow cytometry analysis

Murine organoids were harvested with ice-cold complete adDMEMF/12. After centrifugation at 250 × *g* for 5 min at 4°C, the supernatant was aspirated and discarded, then 1× TrypLE (Gibco, Waltham, MA) was added to each tube and incubated for 5 min at 37°C. After vortexing the tubes, up and down pipetting was performed to dissociate the organoids into a single-cell suspension. The cells were washed with complete adDMEMF/12, and then analyzed by flow cytometry to determine eGFP expression levels. Human rectal organoids were dissociated with 0.25% Trypsin/EDTA, fixed with 4% paraformaldehyde for 15 min, and resuspended in PBS. In HEK293T cells expressing 3HA-CFTR, CFTR plasma membrane density was measured in the presence and absence of anti-hCFTR NBs as described previously.[32]

Immunofluorescent staining and imaging

For confocal imaging, murine organoids were observed with an Evos optical microscope. For immunofluorescence staining, organoids were harvested and washed once with ice-cold complete adDMEMF/12. They were fixed for 1 h in 4% paraformaldehyde, permeabilized with 0.5% Triton X-100 for 30 min, and then blocked with 2% fetal bovine serum in PBS for 1 h at RT. Then the organoids were incubated for 2 h at RT with primary antibodies against cytokeratin 8 (Abcam, Cambridge, UK, DSHB, TROMA-I, AB_531826), cytokeratin 5 (Alexa Fluor 647 coupled antibody, Abcam, RRID AB_2728796), and AR (Abcam, AB_10865716). Then organoids were washed with PBS, followed by an incubation with secondary antibodies coupled to an Alexa Fluor 488 (goat anti-rabbit IgG, Thermo Fisher Scientific, RRID: AB_143165) and Alexa Fluor 594 (goat anti-rat IgG, Thermo Fisher Scientific, RRID: AB_10561522) for 1.30 h at RT. DAPI was used to stain nuclear DNA. Organoids were mounted and imaged with a confocal Nikon microscope. Images were processed with ImageJ.

For human intestinal organoids, matrix embedded organoids were fixed with 4% paraformaldehyde for 1 h at 37°C and subsequently washed with 1× PBS. Next, organoids were permeabilized with 0.1% Triton X-100 in PBS and incubated for 30 min at 37°C, followed by a rinse with 1× PBS. After a blocking step of 2 h with 3% BSA, the organoids were incubated with an anti-calnexin primary monoclonal antibody (Thermo Fisher Scientific, MA3-027) overnight at 37°C. The next day, after a wash step, the sample was incubated with the secondary antibody (goat anti-mouse Alexa Fluor 488) for 4 h at RT. Subsequently, organoids were stained with *Phalloidin* CruzFluor 647 (Santa Cruz Biotechnology) or Hoechst 33342 (2.5 μg/mL in PBS, Sigma-Aldrich) for 2 h at 37 °C. After rinsing, the organoids are ready for two-photon fluorescence microscopy.

The human prostate organoids were treated as above but staining were performed with anti-TOM20 (BD Transduction Laboratories), Phalloidin-Alexa Fluor 546 (Thermo Fisher Scientific), and DAPI. z stacks (350 μm) were acquired with a confocal microscope (Leica TCS SP8 X) equipped with a Mai Tai DeepSee multiphoton laser (Spectra-Physics) and a 40× long-working distance objective (HC PL IRAPO ×40/1.10 W CORR). Emission light was detected with hybrid refractive light detectors (HyD RLD, Leica).

Determination of NB toxicity on organoid development

The number of murine organoids was determined using a counting cell at 9 days after incubation with NBs and reseeding the cells in the respective organoid cultures.

The number of human rectal organoids was determined by automated counting of organoids in one picture 14 days after incubation with NBs and reseeding the cells in the respective organoid cultures. Replicates were obtained from different wells in one experiment and two independent experiments were performed.

Size distribution of organoids

Bright-field images were obtained on an EVOS fl AMF-4306 AMG microscope. The images were analyzed with the software CellProfiler. The morphological parameters of organoids were extracted with the MeasureObjectSizeShape module of CellProfiler. For in-depth analysis, we used the open source KNIME Analytics Platform.

Detection of NB-mediated on-target gene-editing efficiency

After incubation with NBs, murine organoids were grown for 9 days. gDNA was extracted using a gDNA extraction kit (Macherey-Nagel). Primers were designed to amplify approximately 400–700 bp of the region targeted by the guide RNAs (Table S5). gDNA (50 ng) was used for PCR amplification. The size of the PCR fragments was checked using an agarose gel. PCR fragments were then purified using a gel extraction kit (New England Biolabs) and subjected to Sanger sequencing. Sequencing results were analyzed for the percentage of INDEL using ICE (https://ice.synthego.com/#/) or DECODR (https://decodr.org/).

Off-target genome editing detection

The potential off-target sites for the guide RNAs used in this study were determined using Cas-OFFinder (http://www.rgenome.net/cas-offinder/). Some of the off-target sites with two or three mismatches for each guide RNA were selected for further analysis. Note, only off-target sites with a PAM sequence (NGG) were tested here. PCR primers were designed to amplify a fragment of about 400–700 bp flanking the identified potential off-target sites (Table S5). gDNA was isolated and the PCR and fragment isolation were performed as mentioned above. The PCR fragments were then sequenced by Sanger sequencing. Sequencing results were analyzed for the percentage of INDELs using ICE (https://ice.synthego.com/#/) and DECODR (https://decodr.org/).

Statistical analysis

The t test was used for two-group comparison followed by non-parametric Mann-Whitney test. One-way ANOVA followed by Tukey's multiple comparisons test was used for multi-group comparison if the data obeyed the normal distribution. In the case that the data did not obey the normal distribution, Mann-Whitney test was used for two-group comparison and Kruskal-Wallis test was used for multi-group comparison. The statistical tests applied are indicated in the figure legends.

DATA AVAILABILITY

All data including Sanger sequencing data supporting the conclusions of this article are available from the corresponding author upon request.

SUPPLEMENTAL INFORMATION

Supplemental information can be found online at https://doi.org/10.1016/j.omtn.2023.06.004.

ACKNOWLEDGMENTS

Funding was received from the CHEMAAV (ANR-19-CE18-0001) grant operated by the French National Research Agency (ANR). This study was supported by research funding (CRISPR screen Action) from the Canceropôle Provence-Alpes-Côte d'Azur, the French National Cancer Institute (INCa), and the Provence-Alpes-côte d'Azur Region. A.K. and V.T. received a PhD fellowship from the French Ministry of Research. M.B. and M.M.E. are supported by FWO-SB (Flemish Research Foundation) doctoral fellowships, 1SE8122N and 1S29917N, respectively, M.S.C. by a senior post-doctoral FWO scholarship 12Z5920N and KU Leuven BOFZAP professorship. Cystic Fibrosis Research is funded by the Belgian CF patient Association and Fund Alphonse Jean Forton from the King Baudouin Foundation (2020-J1810150-E015) and by FWO (SBO OrganID: S001221N). We are very grateful to the Foundation Hubrecht Organoid Technology (HUB) for sharing human breast cancer organoid models.

AUTHOR CONTRIBUTIONS

V.T. and A.K. were responsible for experimental design, methodology, experiments, analysis, and preparation of the first draft of the manuscript. E.B., M.B., M.M.E., M.H.G., D.H., F.L., A.G.-G., L.M., and M.K. were responsible for designing, performing, and analyzing experiments. F.V. and P.E.M. provided materials and advice. R.G., M.S.C., H.C., and A.C.R. were involved in design and supervision of the human organoid experiments, software analysis, and in the review and editing of the paper. Y.C. provided the human prostate organoids and culture protocols. F.B. was involved design, funding acquisition, supervision of the murine organoid experiments in the review, and editing of the paper. E.V. designed the project, supervised the work, performed experiments, discussed and analyzed results, and wrote the manuscript.

DECLARATION OF INTERESTS

P.E.M. is an inventor on a patent relating to the NBs technology (patent WO 2017/068077). E.V. is an inventor on the patent on pseudotyping of retroviral particles with BaEV envelope glycoproteins (patent WO 07290918.7). H.C. is affiliated with Roche but has no financial interests to declare.

REFERENCES

1. Zhao, S., Wu, X., Tan, Z., Ren, Y., Li, L., Ou, J., Lin, Y., Song, H., Feng, L., Seto, D., et al. (2023). Generation of human embryonic stem cell-derived lung organoids for modeling infection and replication differences between human adenovirus types 3 and 55 and evaluating potential antiviral drugs. J. Virol. *97*, e0020923. https://doi.org/10.1128/jvi.00209-23.

2. Boonekamp, K.E., Heo, I., Artegiani, B., Asra, P., van Son, G., de Ligt, J., and Clevers, H. (2021). Identification of novel human Wnt target genes using adult endodermal tissue-derived organoids. Dev. Biol. *474*, 37–47. https://doi.org/10.1016/j.ydbio.2021.01.009.

3. Yousef Yengej, F.A., Jansen, J., Ammerlaan, C.M.E., Dilmen, E., Pou Casellas, C., Masereeuw, R., Hoenderop, J.G., Smeets, B., Rookmaaker, M.B., Verhaar, M.C., and Clevers, H. (2023). Tubuloid culture enables long-term expansion of functional human kidney tubule epithelium from iPSC-derived organoids. Proc. Natl. Acad. Sci. USA *120*. e2216836120. https://doi.org/10.1073/pnas.2216836120.

4. Choi, J., Shin, E., Lee, J., Devarasou, S., Kim, D., Shin, J.H., Choi, J.-H., Heo, W.D., and Han, Y.-M. (2023). Light-stimulated insulin secretion from pancreatic islet-like organoids derived from human pluripotent stem cells. Mol. Ther. *31*, 1480–1495. https://doi.org/10.1016/j.ymthe.2023.03.013.

5. Drost, J., Karthaus, W.R., Gao, D., Driehuis, E., Sawyers, C.L., Chen, Y., and Clevers, H. (2016). Organoid culture systems for prostate epithelial and cancer tissue. Nat. Protoc. *11*, 347–358. https://doi.org/10.1038/nprot.2016.006.

6. Clevers, H. (2016). Modeling development and disease with organoids. Cell *165*, 1586–1597. https://doi.org/10.1016/j.cell.2016.05.082.

7. Matano, M., Date, S., Shimokawa, M., Takano, A., Fujii, M., Ohta, Y., Watanabe, T., Kanai, T., and Sato, T. (2015). Modeling colorectal cancer using CRISPR-Cas9–mediated engineering of human intestinal organoids. Nat. Med. *21*, 256–262. https://doi.org/10.1038/nm.3802.

8. Dutta, D., Heo, I., and Clevers, H. (2017). Disease modeling in stem cell-derived 3D organoid systems. Trends Mol. Med. *23*, 393–410. https://doi.org/10.1016/j.molmed.2017.02.007.

9. Drost, J., van Boxtel, R., Blokzijl, F., Mizutani, T., Sasaki, N., Sasselli, V., de Ligt, J., Behjati, S., Grolleman, J.E., van Wezel, T., et al. (2017). Use of CRISPR-modified human stem cell organoids to study the origin of mutational signatures in cancer. Science *358*, 234–238. https://doi.org/10.1126/science.aao3130.

10. Schwank, G., Koo, B.-K., Sasselli, V., Dekkers, J.F., Heo, I., Demircan, T., Sasaki, N., Boymans, S., Cuppen, E., van der Ent, C.K., et al. (2013). Functional repair of CFTR by CRISPR/Cas9 in intestinal stem cell organoids of cystic fibrosis patients. Cell Stem Cell *13*, 653–658. https://doi.org/10.1016/j.stem.2013.11.002.

11. Fujii, M., Matano, M., Nanki, K., and Sato, T. (2015). Efficient genetic engineering of human intestinal organoids using electroporation. Nat. Protoc. *10*, 1474–1485. https://doi.org/10.1038/nprot.2015.088.

12. Artegiani, B., van Voorthuijsen, L., Lindeboom, R.G.H., Seinstra, D., Heo, I., Tapia, P., López-Iglesias, C., Postrach, D., Dayton, T., Oka, R., et al. (2019). Probing the tumor suppressor function of BAP1 in CRISPR-engineered human liver organoids. Cell Stem Cell *24*, 927–943.e6. https://doi.org/10.1016/j.stem.2019.04.017.

13. Artegiani, B., Hendriks, D., Beumer, J., Kok, R., Zheng, X., Joore, I., Chuva de Sousa Lopes, S., van Zon, J., Tans, S., and Clevers, H. (2020). Fast and efficient generation of knock-in human organoids using homology-independent CRISPR–Cas9 precision genome editing. Nat. Cell Biol. *22*, 321–331. https://doi.org/10.1038/s41556-020-0472-5.

14. Hofer, M., and Lutolf, M.P. (2021). Engineering organoids. Nat. Rev. Mater. *6*, 402–420. https://doi.org/10.1038/s41578-021-00279-y.

15. Geurts, M.H., de Poel, E., Pleguezuelos-Manzano, C., Oka, R., Carrillo, L., Andersson-Rolf, A., Boretto, M., Brunsveld, J.E., van Boxtel, R., Beekman, J.M., and Clevers, H. (2021). Evaluating CRISPR-based prime editing for cancer modeling and CFTR repair in organoids. Life Sci. Alliance *4*, e202000940. https://doi.org/10.26508/lsa.202000940.

16. Doudna, J.A., and Charpentier, E. (2014). The new frontier of genome engineering with CRISPR-Cas9. Science *346*, 1258096. https://doi.org/10.1126/science.1258096.

17. Gaj, T., Gersbach, C.A., and Barbas, C.F. (2013). ZFN, TALEN, and CRISPR/Cas-based methods for genome engineering. Trends Biotechnol. *31*, 397–405. https://doi.org/10.1016/j.tibtech.2013.04.004.

18. Hustedt, N., and Durocher, D. (2016). The control of DNA repair by the cell cycle. Nat. Cell Biol. *19*, 1–9. https://doi.org/10.1038/ncb3452.

19. Heckl, D., Kowalczyk, M.S., Yudovich, D., Belizaire, R., Puram, R.V., McConkey, M.E., Thielke, A., Aster, J.C., Regev, A., and Ebert, B.L. (2014). Generation of mouse models of myeloid malignancy with combinatorial genetic lesions using CRISPR-Cas9 genome editing. Nat. Biotechnol. *32*, 941–946. https://doi.org/10.1038/nbt.2951.

20. Mandal, P.K., Ferreira, L.M.R., Collins, R., Meissner, T.B., Boutwell, C.L., Friesen, M., Vrbanac, V., Garrison, B.S., Stortchevoi, A., Bryder, D., et al. (2014). Efficient ablation of genes in human hematopoietic stem and effector cells using CRISPR/Cas9. Cell Stem Cell *15*, 643–652. https://doi.org/10.1016/j.stem.2014.10.004.

21. Hendel, A., Bak, R.O., Clark, J.T., Kennedy, A.B., Ryan, D.E., Roy, S., Steinfeld, I., Lunstad, B.D., Kaiser, R.J., Wilkens, A.B., et al. (2015). Chemically modified guide RNAs enhance CRISPR-Cas genome editing in human primary cells. Nat. Biotechnol. *33*, 985–989. https://doi.org/10.1038/nbt.3290.

22. Dawei, S., LewisD, E., and Emma, L.,R. (2020). Organoid Easytag: An Efficient Workflow for Gene Targeting in Human Organoids (The Company of Biologists preLights). https://doi.org/10.1242/prelights.20966.

23. de Poel, E., Spelier, S., Hagemeijer, M.C., van Mourik, P., Suen, S.W.F., Vonk, A.M., Brunsveld, J.E., Ithakisiou, G.N., Kruisselbrink, E., Oppelaar, H., et al. (2023). FDA-approved drug screening in patient-derived organoids demonstrates potential of drug repurposing for rare cystic fibrosis genotypes. J. Cyst. Fibros. *22*, 548–559. https://doi.org/10.1016/j.jcf.2023.03.004.

24. Karthaus, W.R., Iaquinta, P.J., Drost, J., Gracanin, A., van Boxtel, R., Wongvipat, J., Dowling, C.M., Gao, D., Begthel, H., Sachs, N., et al. (2014). Identification of multipotent luminal progenitor cells in human prostate organoid cultures. Cell *159*, 163–175. https://doi.org/10.1016/j.cell.2014.08.017.

25. Mangeot, P.E., Risson, V., Fusil, F., Marnef, A., Laurent, E., Blin, J., Mournetas, V., Massouridès, E., Sohier, T.J.M., Corbin, A., et al. (2019). Genome editing in primary cells and in vivo using viral-derived Nanoblades loaded with Cas9-sgRNA ribonucleoproteins. Nat. Commun. *10*, 45. https://doi.org/10.1038/s41467-018-07845-z.

26. Gutierrez-Guerrero, A., Abrey Recalde, M.J., Mangeot, P.E., Costa, C., Bernadin, O., Périan, S., Fusil, F., Froment, G., Martinez-Turtos, A., Krug, A., et al. (2021). Baboon envelope pseudotyped "nanoblades" carrying cas9/gRNA complexes allow efficient genome editing in human T, B, and CD34+ cells and knock-in of AAV6-encoded donor DNA in CD34+ cells. Front. Genome *3*, 604371. https://doi.org/10.3389/fgeed.2021.604371.

27. Bernadin, O., Amirache, F., Girard-Gagnepain, A., Moirangthem, R.D., Lévy, C., Ma, K., Costa, C., Nègre, D., Reimann, C., Fenard, D., et al. (2019). Baboon envelope LVs efficiently transduced human adult, fetal, and progenitor T cells and corrected SCID-X1 T-cell deficiency. Blood Adv. *3*, 461–475. https://doi.org/10.1182/bloodadvances.2018027508.

28. Girard-Gagnepain, A., Amirache, F., Costa, C., Lévy, C., Frecha, C., Fusil, F., Nègre, D., Lavillette, D., Cosset, F.-L., and Verhoeyen, E. (2014). Baboon envelope pseudotyped LVs outperform VSV-G-LVs for gene transfer into early-cytokine-stimulated and resting HSCs. Blood *124*, 1221–1231. https://doi.org/10.1182/blood-2014-02-558163.

29. Sato, T., Stange, D.E., Ferrante, M., Vries, R.G.J., van Es, J.H., van den Brink, S., van Houdt, W.J., Pronk, A., van Gorp, J., Siersema, P.D., and Clevers, H. (2011). Long-term expansion of epithelial organoids from human colon, adenoma, adenocarcinoma, and barrett's epithelium. Gastroenterology *141*, 1762–1772. https://doi.org/10.1053/j.gastro.2011.07.050.

30. Moran, O. (2010). Model of the cAMP activation of chloride transport by CFTR channel and the mechanism of potentiators. J. Theor. Biol. *262*, 73–79. https://doi.org/10.1016/j.jtbi.2009.08.032.

31. Vidović, D., Carlon, M.S., da Cunha, M.F., Dekkers, J.F., Hollenhorst, M.I., Bijvelds, M.J.C., Ramalho, A.S., Van den Haute, C., Ferrante, M., Baekelandt, V., et al. (2016). rAAV-cftr∂r rescues the cystic fibrosis phenotype in human intestinal organoids and cystic fibrosis mice. Am. J. Respir. Crit. Care Med. *193*, 288–298. https://doi.org/10.1164/rccm.201505-0914OC.

32. Ensinck, M., De Keersmaecker, L., Heylen, L., Ramalho, A.S., Gijsbers, R., Farré, R., De Boeck, K., Christ, F., Debyser, Z., and Carlon, M.S. (2020). Phenotyping of rare CFTR mutations reveals distinct trafficking and functional defects. Cells *9*, E754. https://doi.org/10.3390/cells9030754.

33. Okamoto, T., Natsume, Y., Yamanaka, H., Fukuda, M., and Yao, R. (2021). A protocol for efficient CRISPR-Cas9-mediated knock-in in colorectal cancer patient-derived organoids. STAR Protoc. *2*, 100780. https://doi.org/10.1016/j.xpro.2021.100780.

34. Son, J.S., Park, C.-Y., Lee, G., Park, J.Y., Kim, H.J., Kim, G., Chi, K.Y., Woo, D.-H., Han, C., Kim, S.K., et al. (2022). Therapeutic correction of hemophilia A using 2D endothelial cells and multicellular 3D organoids derived from CRISPR/Cas9-engineered patient iPSCs. Biomaterials *283*, 121429. https://doi.org/10.1016/j.biomaterials.2022.121429.

35. Ogawa, J., Pao, G.M., Shokhirev, M.N., and Verma, I.M. (2018). Glioblastoma model using human cerebral organoids. Cell Rep. *23*, 1220–1229. https://doi.org/10.1016/j.celrep.2018.03.105.

36. Gu, W., Colarusso, J.L., Dame, M.K., Spence, J.R., and Zhou, Q. (2022). Rapid establishment of human colonic organoid knockout lines. STAR Protoc. *3*, 101308. https://doi.org/10.1016/j.xpro.2022.101308.

37. Drost, J., van Jaarsveld, R.H., Ponsioen, B., Zimberlin, C., van Boxtel, R., Buijs, A., Sachs, N., Overmeer, R.M., Offerhaus, G.J., Begthel, H., et al. (2015). Sequential cancer mutations in cultured human intestinal stem cells. Nature *521*, 43–47. https://doi.org/10.1038/nature14415.

38. Menche, C., and Farin, H.F. (2021). Strategies for genetic manipulation of adult stem cell-derived organoids. Exp. Mol. Med. *53*, 1483–1494. https://doi.org/10.1038/s12276-021-00609-8.

39. Hendriks, D., Artegiani, B., Hu, H., Chuva de Sousa Lopes, S., and Clevers, H. (2021). Establishment of human fetal hepatocyte organoids and CRISPR-Cas9-based gene knockin and knockout in organoid cultures from human liver. Nat. Protoc. *16*, 182–217. https://doi.org/10.1038/s41596-020-00411-2.

40. Tucci, F., Galimberti, S., Naldini, L., Valsecchi, M.G., and Aiuti, A. (2022). A systematic review and meta-analysis of gene therapy with hematopoietic stem and progenitor cells for monogenic disorders. Nat. Commun. *13*, 1315. https://doi.org/10.1038/s41467-022-28762-2.

41. Sun, D., Evans, L., Perrone, F., Sokleva, V., Lim, K., Rezakhani, S., Lutolf, M., Zilbauer, M., and Rawlins, E.L. (2021). A functional genetic toolbox for human tissue-derived organoids. Elife *10*, e67886. https://doi.org/10.7554/eLife.67886.

42. Lino, C.A., Harper, J.C., Carney, J.P., and Timlin, J.A. (2018). Delivering CRISPR: a review of the challenges and approaches. Drug Deliv. *25*, 1234–1257. https://doi.org/10.1080/10717544.2018.1474964.

43. Banskota, S., Raguram, A., Suh, S., Du, S.W., Davis, J.R., Choi, E.H., Wang, X., Nielsen, S.C., Newby, G.A., Randolph, P.B., et al. (2022). Engineered virus-like particles for efficient in vivo delivery of therapeutic proteins. Cell *185*, 250–265.e16. https://doi.org/10.1016/j.cell.2021.12.021.

44. Xie, Q., Liu, Y., Cai, T., Horton, C., Stefanson, J., and Wang, Z.A. (2017). Dissecting cell-type-specific roles of androgen receptor in prostate homeostasis and regeneration through lineage tracing. Nat. Commun. *8*, 14284. https://doi.org/10.1038/ncomms14284.

45. Jefremow, A., Neurath, M.F., and Waldner, M.J. (2021). CRISPR/Cas9 in gastrointestinal malignancies. Front. Cell Dev. Biol. *9*, 727217. https://doi.org/10.3389/fcell.2021.727217.

46. Lõhmussaar, K., Kopper, O., Korving, J., Begthel, H., Vreuls, C.P.H., van Es, J.H., and Clevers, H. (2020). Assessing the origin of high-grade serous ovarian cancer using CRISPR-modification of mouse organoids. Nat. Commun. *11*, 2660. https://doi.org/10.1038/s41467-020-16432-0.

47. Vonk, A.M., van Mourik, P., Ramalho, A.S., Silva, I.A.L., Statia, M., Kruisselbrink, E., Suen, S.W.F., Dekkers, J.F., Vleggaar, F.P., Houwen, R.H.J., et al. (2020). Protocol for application, standardization and validation of the forskolin-induced swelling assay in cystic fibrosis human colon organoids. STAR Protoc. *1*, 100019. https://doi.org/10.1016/j.xpro.2020.100019.

48. Maurice, M., Verhoeyen, E., Salmon, P., Trono, D., Russell, S.J., and Cosset, F.-L. (2002). Efficient gene transfer into human primary blood lymphocytes by

surface-engineered lentiviral vectors that display a T cell–activating polypeptide. Blood *99*, 2342–2350. https://doi.org/10.1182/blood.V99.7.2342.

49. Levy, C., Fusil, F., Amirache, F., Costa, C., Girard-Gagnepain, A., Negre, D., Bernadin, O., Garaulet, G., Rodriguez, A., Nair, N., et al. (2016). Baboon envelope pseudotyped lentiviral vectors efficiently transduce human B cells and allow active factor IX B cell secretion in vivo in NOD/SCIDγc-/- mice. J. Thromb. Haemostasis *14*, 2478–2492. https://doi.org/10.1111/jth.13520.

50. Dekkers, J.F., Wiegerinck, C.L., de Jonge, H.R., Bronsveld, I., Janssens, H.M., de Winter-de Groot, K.M., Brandsma, A.M., de Jong, N.W.M., Bijvelds, M.J.C., Scholte, B.J., et al. (2013). A functional CFTR assay using primary cystic fibrosis intestinal organoids. Nat. Med. *19*, 939–945. https://doi.org/10.1038/nm.3201.

51. Frecha, C., Costa, C., Nègre, D., Gauthier, E., Russell, S.J., Cosset, F.-L., and Verhoeyen, E. (2008). Stable transduction of quiescent T cells without induction of cycle progression by a novel lentiviral vector pseudotyped with measles virus glycoproteins. Blood *112*, 4843–4852. https://doi.org/10.1182/blood-2008-05-155945.